Solar Energy Materials & Solar Cells 103 (2012) 76–79

Contents lists available at SciVerse ScienceDirect

Solar Energy Materials & Solar Cells

journal homepage: www.elsevier.com/locate/solmat

Fully spray-coated inverted organic solar cells

Jae-Wook Kang [a,*], Yong-Jin Kang [a,b], Sunghoon Jung [a], Myungkwan Song [a], Do-Geun Kim [a], Chang Su Kim [a], Soo H. Kim [b]

[a] Department of Surface Technology, Korea Institute of Materials Science (KIMS), Changwon 641-831, Republic of Korea
[b] Department of Nanosystem and Nanoprocess Engineering, Pusan National University, Busan 609-735, Republic of Korea

ARTICLE INFO

Article history:
Received 3 March 2012
Received in revised form
10 April 2012
Accepted 14 April 2012

Keywords:
Organic solar cell
Spray coating process
Large-area

ABSTRACT

This study evaluated the possibility of utilizing a spray-coating method for all spray-coated inverted organic solar cells (IOSCs). The spray-coating process was applied to deposit electron selective, active and hole selective layers. The IOSCs fabricated by fully spray-coating method showed a power conversion efficiency of 3.17 and 1.33% at a cell area of 0.36 and 15.25 cm^2, respectively, under AM.1.5 simulated illumination, resulting in similar performances with that of spin-coated devices.

1. Introduction

Development in the field of organic solar cells (OSCs) has been growing due to low production costs and roll-to-roll manufacturing on flexible substrate [1–8]. In recent years, the organic solar cell systems, poly(3-hexylthiophene) (P3HT) as electron donor and: [6,6]-phehyl-C61 butyric acid methyl ester (PCBM) as electron acceptor blends have been made and power conversion efficiency (PCE) of up to 5–6% [9–11] Recently the highest PCE of 10.6% was successfully demonstrated a solution-processed tandem organic solar cells [12]. For solution processed cells, mostly OSC layers are fabricated by spin-coating method, however, it is not suitable for roll-to-roll fabrication and has large materials losses with a limited substrate size [6]. To overcome these problems, several groups have explored various coating techniques such as doctor blading, [13] screen printing, [14] and inkjet printing [15,16] and spray-coating [17–21].

The spray-coating technique with potential advantages of enabling a no-limitation in substrate size and low utilization of polymers can be a promising substitute for overcoming the drawbacks of the conventional spin-coating process. Outstanding of these merits, spray-coating method has been developed for the fabrication of OSCs with many advantages, such as large-area coating, uniform coating, roll-to-roll compatible and low-cost process [17,18]. Furthermore, the spray-coating method is able to access a broad spectrum of fluids with various rheologies, offering the opportunity to tune the system to deposit practically almost any kind of solution and obtain the desired film properties [20]. Recently, spray-coating technologies have been reported the fabrication of conventional OSCs structure (ITO/hole selective layer/active layer/Al) and inverted OSCs (IOSCs) structure (ITO/electron selective layer/active layer/hole selective layer/Ag) focused on controlling the surface roughness and coating thickness of hole selective and active layers, resulting in similar device performance with spin-coated OSCs [17,19–25].

For the fabrication of all-printed OSCs, an inverted architecture is usually used to avoid the vacuum process for the deposition of the low-work function metal electrode (such as Al and Ca) in which a high work function anode (such as Ag and Au) to collect holes and electron selective layer on the surface of ITO to collect electrons are utilized [26–29]. One critical issue in this fabrication process is how to form hole selective layer, poly(3.4-ethylenedioxythiophene):poly(styrene-sulfonate) (PEDOT:PSS), on top of active layer by using spray-coating process with a good film quality. PEDOT:PSS was not coated well onto active layer because PEDOT:PSS aqueous solution is highly hydrophilic and P3HT:PCBM film is hydrophobic, resulting in very poor device performance.

This paper reports the fabrication of inverted OSCs (IOSCs) with a ITO/ZnO/P3HT:PCBM/PEDOT:PSS/Ag structure utilizing fully spray-coated electron selective, active and hole selective layers to demonstrate large-area, air-stable and highly efficient devices. The effects of the spray-coated layers on the device performance and life time were investigated, and the performance of the IOSCs with fully spray-coated layers was then compared with that of the all spin-coated device.

2. Experimental details

The IOSCs fabricated on the ITO-coated glass with a sheet resistance of ~10 Ω/sq. First, ITO substrates underwent a routine

* Corresponding author. Tel.: +82 55 280 3572; fax: +82 55 280 3570.
E-mail address: jwkang@kims.re.kr (J.-W. Kang).

0927-0248/$ - see front matter © 2012 Elsevier B.V. All rights reserved.
http://dx.doi.org/10.1016/j.solmat.2012.04.027

cleaning procedure, which included sonication and repeated rinsing in acetone and isopropyl alcohol. The substrates were then dried in an oven at 120 °C and treated with UV-ozone for 5 min. The spray-coating conditions for three layers were optimized to minimize the surface roughness by varying the solution injection rate, carrier gas flow, nozzle to substrate distance and printing speed. In this study, the carrier gas flow and printing speed was optimized as 50 psi, and 6 cm/min at *x*-axis and 1800 cm/min at *y*-axis for the spray-coating of three layers, respectively.

For the preparation of the ZnO sol–gel solution, zinc acetate (16.40 mg, Aldrich) was dissolved in 2-methoxyethanol (100 ml, Aldrich) using a magnetic stirrer. Ethanolamine (5 ml, Aldrich) was then added to the zinc acetate solution and the resulting solution was kept at 60 °C for 1 h under ambient conditions with vigorous stirring. Before spray-coating, the ZnO solution was diluted with methanol (ZnO sol–gel: methanol=1:10) because a solution without dilution was not well distributed from the nozzle or the layer was not coated uniformly. The ZnO thin film as electron selective layer was spray-coated on ITO glass with a thickness of approximately 40 nm (in an injection rate of 0.5 ml/min and nozzle to substrate distance of 8.5 cm), followed by thermal annealing at 300 °C for 10 min. The P3HT:PCBM blend solution was prepared at 1:1 mass ratio in 1,2-dichlorobenzene (10 mg/ml P3HT and 10 mg/ml PCBM). The photoactive materials were spray-coated with a thickness of 180–320 nm in an injection rate of 0.2 ml/min and nozzle to substrate distance of 3.5 cm. Slow evaporation and pre-annealing (150 °C for 20 min on hot plate) were carried out in a glove box. A buffer layer of PEDOT:PSS (AI 4083, Stark):isopropyl alcohol (IPA) (PEDOT:PSS:IPA=1:6) was prepared using spray-coating with an injection rate of 0.5 ml/min and nozzle to substrate distance of 5 cm after passing through a 0.45 μm filter with a thickness of approximately 20–100 nm on the temperature of 25–80 °C. The coated PEDOT:PSS film was dried at 150 °C for 1 min on a hot plate in a glove box. In control device, the 40-nm-thick ZnO, 270-nm-thick P3HT:PCBM and 40-nm-thick PEDOT:PSS layers were spin-coated with a spin speed of 1000, 600 and 5000 rpm for 40 s, respectively. Finally, a 120-nm-thick Ag electrode was evaporated at 3×10^{-6} Torr. The effective area of the active layer for the solar cell prepared in this approach was 0.36 cm^2, which was determined using a shadow mask. The fabricated IOSCs was characterized using restricted illumination by inserting a shadow mask to eliminate excess photocurrent from conductive PEDOT:PSS layer [30]. The current–voltage (*J–V*) characteristics were measured under AM 1.5 simulated illumination with an intensity of 100 mW/cm^2 (Pecell Technologies Inc., PEC-L11 model). The intensity of sunlight illumination was calibrated using a standard Si photodiode detector with a KG-5 filter. The *J–V* curves were recorded automatically with a Keithley SMU 2400 source meter by illuminating the IOSCs.

3. Results and discussion

A schematic diagram of the spray-coating apparatus is shown in Fig. 1(a). The spray-coating system has two nozzles as the core and clad. The core nozzle was connected to the injection pump for the solution (ZnO, P3HT:PCBM or PEDOT:PSS) and the clad nozzle was linked an N_2 for the carrier gas. A computer controlled *xy*-stage (nozzle and substrate moving stage) and injection pump allows a reproducible thickness of the deposited film [22,25]. The spray-coating conditions were optimized to minimize the surface roughness. The stage was vacuumed on top of hot-stage to control of substrate temperature. To compare the surface morphologies of each layer, atomic force microscopy (AFM) images were taken as

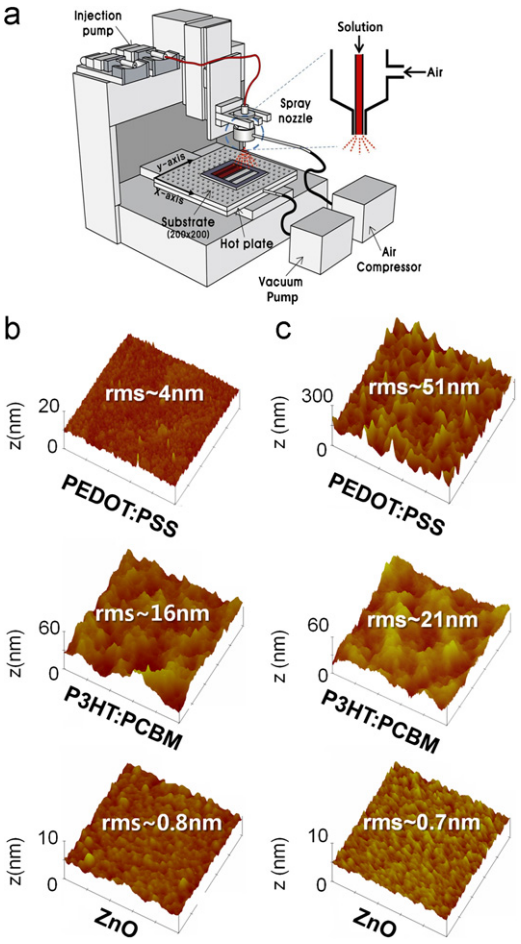

Fig. 1. (a) Schematic diagram of the spray-coating apparatus. AFM images and rms roughness of the three different layers in the inverted organic solar cell coated by (b) spin- and (c) spray-coating process. AFM image scans are 5 × 5 μm.

shown in Fig. 1(b) and (c). The surface morphology and roughness of ZnO and P3HT:PCBM layers prepared by spray-coating method at 25 °C were similar in spin-coated layers. To form uniform PEDOT:PSS film on top of P3HT:PCBM layer in spray-coating process, the PEDOT:PSS was mixed with IPA solution and the substrate was heated up to 80 °C to improve wettability. The surface morphology of the PEDOT:PSS layer in optimized spray-coating process on top of the active layer shows root-mean-square (rms) roughness values of 4 and 51 nm using the spin- and spray-coating process, respectively.

Fig. 2 shows the photovoltaic response IOSCs produced with a different spray-coated P3HT:PCBM thickness with a spray-coated 40-nm-thick ZnO and spin-coated 40-nm-thick PEDOT:PSS. The thickness of the P3HT:PCBM layer in the IOSCs plays a major role in the device performance.[31] With increasing P3HT:PCBM thickness from 180 to 320 nm, the short circuit current density (J_{sc}) of the IOSCs increase from 7.74 to 9.61 mA/cm^2 with a constant open circuit voltage (V_{oc}) of about 0.59 V. The performance of the spray-coated devices does not decrease substantially with thickness and the PCE of the cells remains around 3.0% in the thickness of 270–320 nm. This thickness has relevant industrial applications, since it could increase the production yield and relax the constrains in thickness control [20]. The highest PCE of 3.12% is achieved at 270 nm, where a J_{sc} reaches 9.33 mA/cm^2 and the fill factor (*FF*) is 0.56.

In order to demonstrate fully spray-coated IOSCs, the PEDOT:PSS layer was spray coated onto spray-coated P3HT:PCBM and ZnO layers. Fig. 3 shows the effects of coating temperature on the

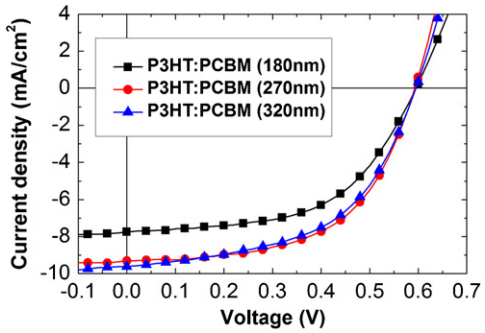

Fig. 2. Comparison of the photovoltaic response of inverted organic solar cells produced by spray-coated P3HT:PCBM layers with a different thickness onto spray-coated 40-nm-thick ZnO layer. The 40-nm-thick PEDOT:PSS was spin-coated.

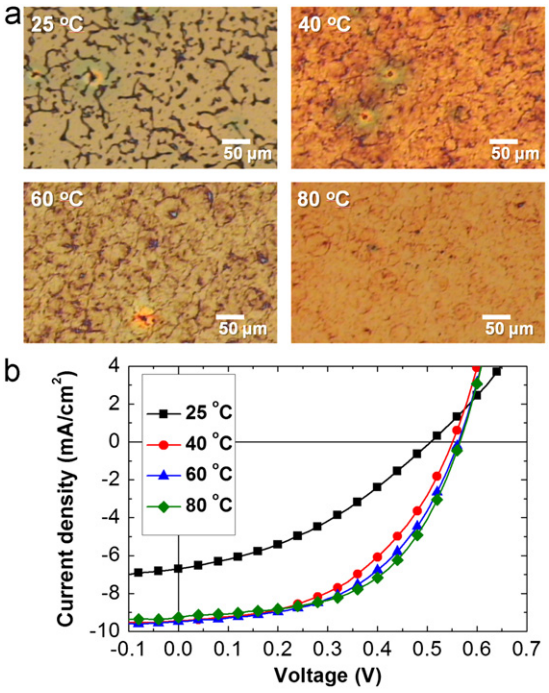

Fig. 3. (a) Optical images of spray-coated PEDOT:PSS layers on top of P3HT:PCBM layer. (b) Comparison of the inverted organic solar cells produced by spray-coated PEDOT:PSS layers with a different coating temperature (with spray-coated 40-nm-thick ZnO and 270-nm-thick P3HT:PCBM layers).

final thin film and device performance. The substrate temperature was varied from 80 °C, close to the boiling point of IPA, to 25 °C. Without heating stage around 25 °C, the PEDOT:PSS solution cannot wet completely onto the active layer and is not able to cover the entire P3HT:PCBM surface as shown in Fig. 3(a), resulting very poor device performance with a PCE of 1.25% shown in Fig. 3(b). The deposition improves at 40 °C, the PEDOT:PSS solution begins to settle into a full film on top of active layer. Further increase of the substrate temperature to 80 °C, allowed a complete film formation of the whole surface, which lead to dramatically improvement of the PCE from 1.25 to 2.93% and decrease of the series resistance (R_s) from 7.12 to 4.35 Ωcm^2. Fig. 4 shows the effects of PEDOT:PSS thickness on device performance with a fixed substrate temperature of 80 °C. In our experiment, the 40-nm-thick PEDOT:PSS coated at 80 °C showed best device performance in fully spray-coated IOSCs with a PCE of 2.93% (J_{sc}=9.18 mA/cm^2, V_{oc}=0.58 V and FF=0.54).

With optimized coating conditions for ZnO, P3HT:PCBM and PEDOT:PSS layers, we could compare the performance of devices

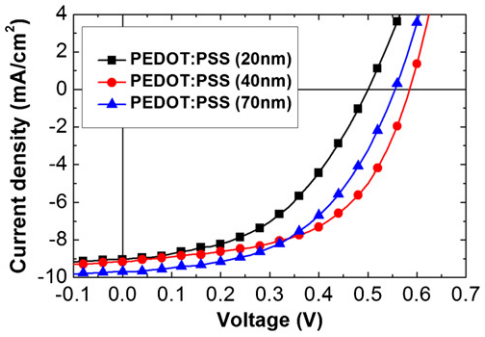

Fig. 4. Comparison of the inverted organic solar cells produced by spray-coated PEDOT:PSS layers at a temperature of 80 °C with a different thickness (with spray-coated 40-nm-thick ZnO and 270-nm-thick P3HT:PCBM layers).

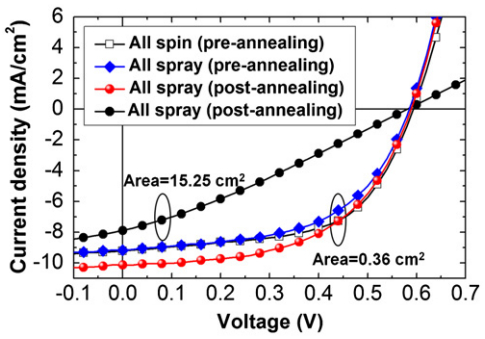

Fig. 5. Comparison of the photovoltaic response of inverted organic solar cells produced with all spin- and spray-coated inverted organic solar cells with different annealing process and device area.

where three layers were selectively replaced from a control fully spin-coated device as shown in Fig. 5. As shown in Fig. 1(c), surface morphology of the spray-coated PEDOT:PSS layer on top of the active layer at 80 °C shows very high rms roughness values of 51 nm. Therefore, in all spray-coated layers, the interface between the P3HT:PCBM and PEDOT:PSS layers was more poor than spin-coated layers, resulting in decreased device performance than spin-coated device. To further optimize the thermal annealing process, we changed the annealing method from pre-annealing to post-annealing in the active layer. After spray-coating of PEDOT:PSS onto active layer, the films were post-annealed at 150 °C for 20 min, resulting in increase of J_{sc} from 9.62 to 10.09 mA/cm^2 and PCE from 2.93 to 3.17% as shown in Fig. 5. It could be caused by the enhancement of interface contact at the PEDOT:PSS and active layer. This result is comparable to that of the all spin-coated (J_{sc}=9.62 mA/cm^2, V_{oc}=0.58 V, FF=0.55 and PCE=3.12%). This demonstrates for the first time a close similar performance in IOSCs between devices produced by fully spin-coating and spray-coating process, a coating technique scalable to fabricate large-area roll-to-roll devices. Furthermore, this process was applied to demonstrate large-area IOSCs with a cell area of 15.25 cm^2, resulting in the PCE of 1.33%. With increasing cell area, the R_s increased significantly from 4.57 to 53.2 Ωcm^2, resulting in high reduction of FF from 0.54 to 0.29. The scale up of the cell area leads to a decrease in PCE caused by an increase in R_s owing to the high sheet resistance of ITO and the difficult optimization of large-area thin film deposition. The R_s can be reduced significantly using the metal-grid electrode onto or below ITO electrode, yielding an improvement of device performance [22,30]. Fig. 6 shows the stability of the IOSCs prepared by fully spin-coating and spray-coating processes. The stability studies were performed in the dark with ambient conditions tested according to ISOS-D-1(shelf) [32].

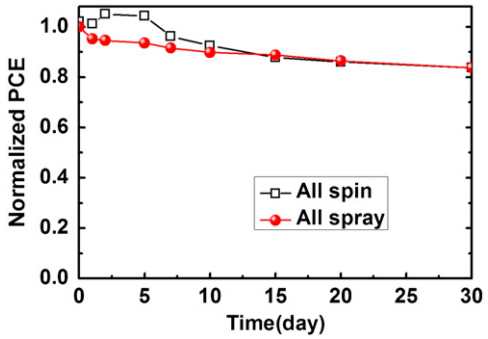

Fig. 6. Normalized PCE of the unencapsulated IOSCs stored for 30 days in air under ambient conditions.

The performance of the IOSCs was evaluated for 30 days. The normalized PCE of the unencapsulated IOSCs with the fully spray-coating process after 30 days showed a similar value of $>80\%$ with the fully spin-coated devices.

4. Conclusion

The spray-coating method was successfully applied to demonstrate fully spray-coated IOSCs with a high device performance, yielding the PCE of 3.17 and 1.33% at a cell area of 0.36 and 15.25 cm^2, respectively. It indicated that the spray-coating method can replace the conventional spin-coating and can be applied to the roll-to-roll process as well as the large-area fabrication.

Acknowledgments

This study was supported by the New and Renewable Energy of the Korea Institute of Energy Technology Evaluation and Planning (KETEP) Grant nos. (2011T100200034 and 20103020010050) funded by the Ministry of the Knowledge Economy, Republic of Korea.

References

[1] M. Manceau, D. Angmo, M. Jorgensen, F.C. Krebs, ITO-free flexible polymer solar cells: From small model devices to roll-to-roll processed large modules, Organic Electronics 12 (2011) 566–574.
[2] G. Dennler, M.C. Scharber, C.J. Brabec, Polymer-fullerene bulk-heterojunction solar cells, Advanced Materials 21 (2009) 1323–1338.
[3] F. Huang, K.-S. Chen, H.-L. Yip, S.K. Hau, O. Acton, Y. Zhang, J. Luo, A.K.-Y. Jen, Development of new conjugated polymers with donor-π-bridge-acceptor side chains for high performance solar cells, Journal of the American Chemical Society 131 (2009) 13886–13887.
[4] H.-L. Yip, S.K. Hau, N.S. Baek, A.K.-Y. Jen, Self-assembled monolayer modified ZnO/metal bilayer cathodes for polymer/fullerene bulk-heterojunction solar cells, Applied Physics Letters 92 (2008) 193313-1–193313-3.
[5] W.-I. Jeong, J. Lee, S.-Y. Park, J.-W. Kang, J.-J. Kim, Reduction of collection efficiency of charge carriers with increasing cell size in polymer bulk heterojunction solar cells, Advanced Functional Materials 21 (2011) 343–347.
[6] F.C. Krebs, Fabrication and processing of polymer solar cells: a review of printing and coating techniques, Solar Energy Materials and Solar Cells 93 (2009) 394–412.
[7] S.-Y. Park, H.-R. Kim, Y.-J. Kang, D.-H. Kim, J.-W. Kang, Organic solar cells employing magnetron sputtered p-type nickel oxide thin film as the anode buffer layer, Solar Energy Materials and Solar Cells 94 (2010) 2332–2336.
[8] S.-I. Na, S.-S. Kim, J. Jo, S.-H. Oh, J. Kim, D.-Y. Kim, Efficient polymer solar cells with surface relief gratings fabricated by simple soft lithography, Advanced Functional Materials 18 (2008) 3956–3963.
[9] G. Li, V. Shrotriya, J. Huang, Y. Yao, T. Moriarty, K. Emery, Y. Yang, High-efficiency solution processable polymer photovoltaic cells by self-organization of polymer blends, Nature Materials 4 (2005) 864–868.
[10] J.Y. Kim, K. Lee, N.E. Coates, D. Moses, T.-Q. Nguyen, M. Dante, A.J. Heeger, Efficient tandem polymer solar cells fabricated by all-solution processing, Science 317 (2007) 222–225.
[11] G. Dennler, M.C. Scharber, C.J. Brabec, Polymer-fullerene bulk-heterojunction solar cells, Advanced Materials 21 (2009) 1323–1338.
[12] G. Li, R. Zhu, Y. Yang, Polymer solar cells, Nature Photonics 6 (2012) 153–161.
[13] P. Schilinsky, C. Waldauf, C.J. Brabec, Performance analysis of printed bulk heterojunction solar cells, Advanced Functional Materials 16 (2006) 1669–1672.
[14] F.C. Krebs, M. Jorgensen, Kion Norrman, Ole Hagemann, Jan Alstrup, Torben D. Nielsen, Jan Fyenbo, Kaj Larsen, Jette Kristensen, A complete process for production of flexible large are a polymer solar cells entirely using screen printing-first public demonstration, Solar Energy Materials and Solar Cells 93 (2009) 422–441.
[15] C.N. Hoth, S.A. Choulis, P. Schilinsky, C.J. Brabec, High photovoltaic performance of inkjet printed polymer:fullerene blends, Advanced Materials 19 (2007) 3973–3978.
[16] T. Aernouts, T. Aleksandrov, C. Girotto, J. Genoe, J. Poortmans, Polymer based organic solar cells using ink-jet printed active layers, Applied Physics Letters 92 (2008) 033306.
[17] D Vak, S.-S. Kim, J. Jo, S.-H. Oh, S.-I. Na, J. Kim, D.-Y. Kim, Fabrication of organic bulk heterojunction solar cells by a spray deposition method for low-cost power generation, Applied Physics Letters 91 (2007) 081102.
[18] K.X. Steirer, M.O. Reese, B.L. Rupert, N. Kopidakis, D.C Olson, R.T. Collins, D.S. Ginley, Ultrasonic spray deposition for production of organic solar cells, Solar Energy Materials and Solar Cells 93 (2009) 447–453.
[19] L.-M. Chen, Z. Hong, W.L. Kwan, C.-H. Lu, Y.-F. Lai, B. Lei, C.-P. Liu, Y. Yang, Multi-source/component spray coating for polymer solar cells, ACS NANO 4 (2011) 4744–4752.
[20] C. Girotto, D. Moia, B.P. Rand, P. Heremans, High-performance organic solar cells with spray-coated hole-transport and active layers, Advanced Functional Materials 21 (2011) 64–72.
[21] C.N. Hoth, R. Steim, P. Schilinsky, S.A. Choulis, S.F. Tedde, O. Hayden, C.J. Brabec, Topographical and morphological aspects of spray coated organic photovoltaics, Organic Electronics 10 (2009) 587–593.
[22] S.-Y. Park, Y.-J. Kang, S. Lee, D.-G. Kim, J.-K. Kim, J.-H. Kim, J.-W. Kang, Spray-coated organic solar cells with large-area of 12.25 cm^2, Solar Energy Materials and Solar Cells 95 (2011) 852–855.
[23] A. Colsmann, M. Reinhard, T.-H. Kwon, C. Kayser, F. Nickel, J. Czolk, U. Lemmer, N. Clark, J. Jasieniak, A.B. Holmes, D. Jones, Inverted semi-transparent organic solar cells with spray coated, surfactant free polymer top-electrodes, Solar Energy Materials and Solar Cells 98 (2012) 118–123.
[24] R.J. Peh, Y. Lu, F. Zhao, C.-L.K. Lee, W.L. Kwan, Vacuum-free processed transparent inverted organic solar cells with spray-coated PEDOT:PSS anode, Solar Energy Materials and Solar Cells 95 (2011) 3579–3584.
[25] Y.-J. Kang, K. Lim, S. Jung, D.-G. Kim, J.-K. Kim, C.-S. Kim, S.H. Kim, J.-W. Kang, Spray-coated ZnO electron transport layer for air-stable inverted organic solar cells, Solar Energy Materials and Solar Cells 96 (2012) 137–140.
[26] F. Zhang, X. Xu, W. Tang, J. Zhang, Z. Zhuo, J. Wang, J. Wang, Z. Xu, Y. Wang, Recent development of the inverted configuration organic solar cells, Solar Energy Materials and Solar Cells 95 (2011) 1785–1799.
[27] M.S. White, D.C. Olson, S.E. Shaheen, N. Kopidakis, D.S. Ginley, Inverted bulk heterojunction organic photovoltaic device using a solution-derived ZnO underlayer, Applied Physics Letters 89 (2006) 143517-1–143517-3.
[28] K. Norrman, M.V. Madsen, S.A. Gevorgyan, F.C. Krebs, Degradation patterns in water and oxygen of an inverted polymer solar cell, Journal of the American Chemical Society 132 (2010) 16883–16892.
[29] S.K. Hau, H.-L. Yip, K. Leong, A.K.-Y. Jen, Spray coating of silver nanoparticle electrodes for inverted polymer solar cells, Organic Electronics 10 (2009) 719–723.
[30] S.-Y. Park, W.-I. Jeong, D.-G. Kim, J.-K. Kim, D.C. Lim, J.H. Kim, J.-J. Kim, J.-W. Kang, Large-area organic solar cells with metal subelectrode on indium tin oxide anode, Applied Physics Letters 96 (2010) 173301-1–173301-3.
[31] L. Zeng, C.W. Tang, S.H. Chen, Effects of active layer thickness and thermal annealing on polythiophene: fullerene bulk heterojunction photovoltaic devices, Applied Physics Letters 97 (2010) 053305-1–053305-3.
[32] M.O. Reese, S.A. Gevorgyan, M. Jørgensen, E. Bundgaard, S.R. Kurtz, D.S. Ginley, D.C. Olson, M.T. Lloyd, P. Morvillo, E.A. Katz, A. Elschner, O. Haillant, T.R. Currier, V. Shrotriya, M. Hermenau, M. Riede, K.R. Kirov, G. Trimmel, T. Rath, O. Inganas, F. Zhang, M. Andersson, K. Tvingstedt, M. Lira-Cantu, D. Laird, C. McGuiness, S.J. Gowrisanker, M. Pannone, M. Xiao, J. Hauch, R. Steim, D.M. DeLongchamp, Roland Rösch, H. Hoppe, N. Espinosa, A. Urbina, G. Yaman-Uzunoglu, J.-B. Bonekamp, A.J.J.M. van Breemen, C. Girotto, E. Voroshazi, F.C. Krebs, Consensus stability testing protocols for organic photovoltaic materials and devices, Solar Energy Materials and Solar Cells 95 (2011) 1253–1267.